TRANSVERSE AEOLIAN RIDGES NEAR THE TRAVERSE ROUTE OF ZHURONG ROVER. Shangke Tian[1], Zongcheng Ling[1*], Sheng Wan[1], Changqing Liu[1], [1]Shandong Provincial Key Laboratory of Optical Astronomy and Solar-Terrestrial Environment, Institute of Space Sciences, Shandong University, Weihai, Shandong, 264209, China. (zcling@sdu.edu.cn).

Introduction: Transverse Aeolian Ridges (TARs) are one of the aeolian bedforms of Mars, which have been studied by the high spatial resolution orbit data like HiRISE in recent years [1, 3]. They are mainly distributed in low-latitude areas, with a high albedo and symmetrical profiles as their main characteristics [2]. The current research on TARs is mainly based on their morphology and terrestrial simulation area. Only some landing sites have in-situ observation data, such as the landing sites of Opportunity and Curiosity [4, 5], and its formation mechanism remains confused. China's Tianwen-1 mission, the Zhurong rover, has been working for more than 200 Sols and has traveled more than 1,400 meters on the Utopia Planitia. There are a large number of TARs whose albedo is significantly higher than that of the surrounding bedrock on the Utopia Planitia where the travel route of the Zhurong rover is located. The Zhurong rover conducted in-situ investigations on the geological characteristics and compositions of some TARs. Analyzing their compositions and morphology can help to better understand the formation mechanism of these targets, which may help reveal relevant ancient wind activity in the landing area.

Data: The data used in this study are from Tianwen-1 High Resolution Imaging Camera (HiRIC), Navigation and Terrain Camera (NaTeCam), and MRO High Resolution Imaging Science Experiment (HiRISE) Digital Terrain Models (DTMs).

Method: The study area is around the traverse route of the Zhurong rover from May 2021 to October 2021. This work used ArcGIS to draw the TARs features in the area of interest using the HiRIC image as the base map and establish its buffer zone. Subsequently, the HiRISE image and the HiRIC image are georeferenced to obtain the maximum elevation within the range of the TARs elements and the average elevation of the buffer zone and subtract the two to get the TARs height. Moreover, we drew the circumscribed rectangle (minimum area) of the TARs and calculated the length and width of the TARs. In addition, we made panoramic stitching of the navigation camera photos acquired on the same date.

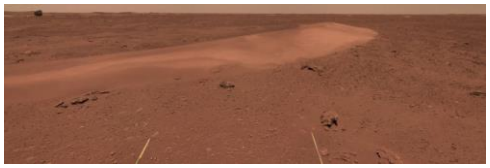

Fig. 1. Panoramic mosaic of TAR navigation cameras in the study area.

Result: In this study, a total of 65 TARs were drawn in the area of interest, which can be roughly divided into barchan, linear, and beaded shapes, as shown in Fig. 2. All TARs are roughly east-west, and the north is the windward side, indicating that the wind direction is roughly from north to south when they are formed. Beaded TARs are the least in the study area, which may indicate that they were active in the TARs in this area. Impact craters exist on a small part of the TARs, indicating that these TARs have been formed for a long time and may have been cemented or diagenetic in origin.

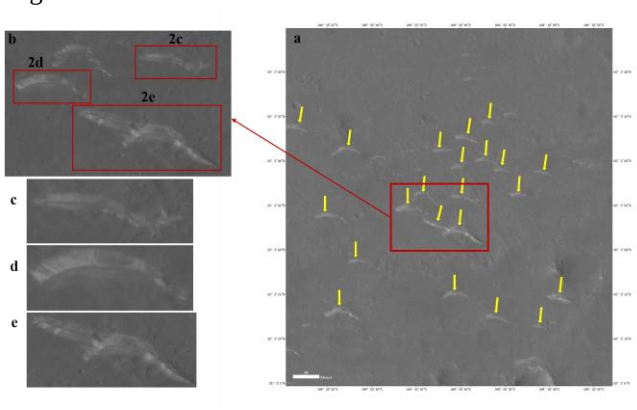

Fig. 2. HiRIC image shows a portion of the TAR of the region of interest. (a) The yellow arrow indicates the wind direction. (b) Three types of TARs in the study area. (c) linear shape. (d) barchan shape. (e) beaded shape.

These TARs are mostly 30-50 meters in width, 10-20 meters in length (Fig. 3b), and 0.3-0.5 meters in height (Fig. 3d). There are several parameters to characterize the distribution of TARs including regular arrangement, and spacing between TARs. The TARs in the region of interest shows roughly the same trend, and the arrangement is disorderly.

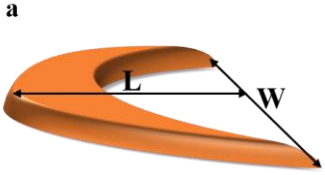

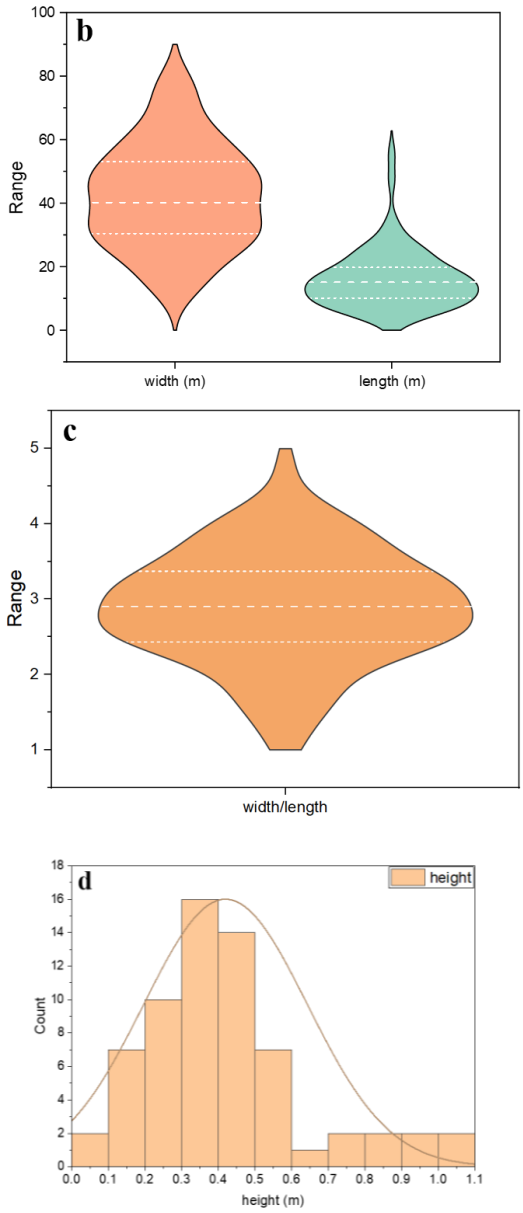

Fig. 3. TARs parameters. (a) Schematic diagram of the TARs, W is the width of the TARs, and L is the length of the TARs. (b) The length and wide distribution of TARs. (c) Range of TARs aspect ratio. (b), (c) The wide dashed line is the median line, The narrow-dashed line ranges from 25% to 75%. (d) Histogram of TARs Height Distribution.

It can be seen from Fig. 4 that the scatter points of TARs in the study area are different from those of the terrestrial dunes and martian dunes [3]. The ratio of height to width (H/W) and the height (H) of the TARs in the study area are both smaller than the values of martian and terrestrial dunes, but they are highly similar to the Mars TARs data points. Therefore, we propose that these landform features are TARs, although they have bright tones and are irregularly arranged.

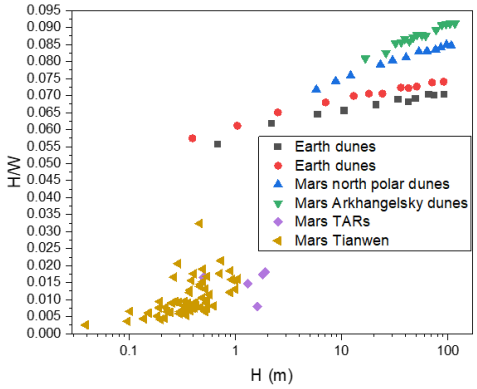

Fig. 4. Comparison of Martian dunes, Mars TARs, Earth dunes, and the study area. The abscissa H is the height, the ordinate H/W is the ratio of height to width. Except for the data in the study area, others are from previous articles [3, 6, 7].

Implication: The TARs in the southern Utopia Plain are very special compared with TARs in other locations on Mars. Studying their genesis and compositions can help to better understand the activities of ancient winds on Mars.

Acknowledgments: We thank the Tianwen-1 payload team for mission operations and China National Space Administration for providing the Tianwen-1 data that made this study possible. This work was supported by the National Natural Science Foundation (U1931211, 11941001, 41972322), and the Natural Science Foundation of Shandong Province (ZR2019MD008). This work is also funded by the Pre-research project on Civil Aerospace Technologies No. D020102 funded by China National Space Administration (CNSA). The Tianwen-1 data used in this work is processed and produced by “Ground Research and Application System（GRAS）of China’s Lunar and Planetary Exploration Program, provided by China National Space Administration (http://moon.bao.ac.cn)”.

References: [1] J. R. Zimbelman. (2010) *Geomorphology*, 121, 22-29. [2] P. E. Geissler. (2014) *JGR*, 119, 2583–2599. [3] E. J. R. Parteli. et al. (2007) *Physical Review E*, 76(4). [4] R. Sullivan. et al. (2005) Nature, 436, 58-61. [5] J. R. Zimbelman and M. Foroutan. (2020) *JGR*, 125. [6] D. C. Berman. (2018) *Icarus*, 312, 247-266. [7] C. H. Hugenholtz. et al. (2017) *Icarus*, 286, 193-201.